2005

Systematic Approach to Design Higher Temperature Composite Pems

T. M. Thampan

N. H. Jalani

P. Choi

Ravindra Datta
Worcester Polytechnic Institute, rdatta@wpi.edu

Journal of The Electrochemical Society, **152** (2) A316-A325 (2005)
0013-4651/2004/152(2)/A316/10/$7.00 © The Electrochemical Society, Inc.

Systematic Approach to Design Higher Temperature Composite PEMs

Tony M. Thampan, Nikhil H. Jalani,* Pyoungho Choi, and Ravindra Datta,z**

Fuel Cell Center, Department of Chemical Engineering, Worcester Polytechnic Institute, Worcester, Massachusetts 01609, USA

The design of higher temperature composite proton-exchange membranes (PEMs) with adequate performance under low relative humidity (RH) is discussed here based on experimental and theoretical considerations. The approach is based on enhancing the acidity and water sorption of a conventional polymer electrolyte membrane by incorporating in it a solid acidic inorganic material. A systematic investigation of the composite Nafion/inorganic additive PEMs based on characterization of water uptake, ion-exchange capacity (IEC), conductivity, and fuel cell polarization is presented. The effects of particle size, chemical treatment, additive loading, and alternate processing methodologies are investigated. The most promising candidate investigated thus far is the nanostructured ZrO_2/Nafion PEM exhibiting an increase of ~10% in IEC, ~40% increase in water sorbed, and ~5% enhancement in conductivity *vs.* unmodified Nafion 112 at 120°C and 40% RH. This appears to be an attractive candidate for incorporation into a membrane-electrode assembly for improved performance under these hot and dry conditions.
 [DOI: 10.1149/1.1843771]

Manuscript submitted February 23, 2004; revised manuscript received July 1, 2004. Available electronically December 23, 2004.

It is fair to say that the commercialization and large-scale deployment of polymer electrolyte membrane (PEM) fuel cells is currently hamstrung by the limitations imposed by the available polymer electrolyte membranes. For instance, Nafion, one of the oldest but still one of the best available PEMs, limits the operating temperature of PEM fuel cells to 80°C on the one hand, thus requiring pure hydrogen as the fuel and consequently imposing severe constraints on reformers, while on the other hand it is still far too expensive, making fuel cells economically unattractive. Unfortunately, the available alternative PEMs compromise performance and longetivity. Thus, there is world-wide effort currently underway to find suitable alternatives to Nafion that might allow higher temperature operation and cost benefit.

This is, however, a particularly challenging task because of the desired performance characteristics. Thus, a good polymer electrolyte membrane must be thin for low resistance, compliant to make a good contact with electrodes but rigid enough to provide support to the membrane electrode assembly (MEA), thermally and dimensionally stable, impervious to gaseous or liquid fuels as well as electrons, must be durable, and should be able to provide excellent proton conductivity rivaling liquid electrolytes (~0.1 S/cm) under hot and dry conditions.

A good proton conductor evidently requires mobile protons. Thus, inorganic proton conductors[1-3] without a liquid phase, while conceptually very attractive, require temperatures in excess of 800°C to provide adequate conductivities via a proton hopping mechanism owing to the high activation energy. At lower temperatures, a liquid-phase for proton conduction is essential, either as a molten or a solvated acid. When a solvent other than water is used, the challenge of complete immobilization of the liquid must be first addressed to ensure stable performance over extended periods. When water is the solvent, the challenge is to retain water within the membrane under hot and dry conditions owing to its high volatility.

An alternate approach, first proposed by Malhotra and Datta,[4] is to incorporate inorganic acidic materials within the conventional polymer electrolytes such as Nafion, in order to improve water retention while simultaneously increasing the number of available acid sites. This approach shows promise for developing PEMs that function adequately at temperatures above 120°C under low relative humidity (RH) conditions,[4] and has consequently become a very active area of research. This paper is concerned with a systematic investigation of the issues related to the design and development of such composite membranes.

* Electrochemical Society Student Member.
** Electrochemical Society Active Member.
z E-mail: rdatta@wpi.edu

Literature Review

A brief literature review of the available ingredients (polymer electrolyte and inorganic additives) for designing composite PEMs is provided below. The available polymer electrolyte membranes may be subdivided into two categories: (*i*) proton-exchange membranes (PEMs), *e.g.*, Nafion, in which the acid anion is covalently attached to the polymer backbone so that only the proton is mobile, requiring a solvent such as water, and (*ii*) polymer-acid complexes (PACs), *e.g.*, PBI/H_3PO_4, in which the acid is simply complexed with a basic membrane so that both the proton and the anion are mobile, *i.e.*, the transference number of protons is less than unity. While a solvent such as water is not essential for conduction in PACs, it aids by further ionizing the acid, but unfortunately can also cause leaching of the acid from the membrane, a serious limitation for long-term stability.

Proton-exchange membranes (PEMs).—Figure 1a shows a schematic of the major components of a proton-exchange membrane, namely the polymer backbone, chemical cross-links, side chains, and the pendant acid group. The right combination of these elements confers the desirable properties listed above. The backbone polymers are: (*i*) fluorinated and (*ii*) hydrocarbon polymers. The common acid groups covalently bound are either: (*i*) sulfonic acid ($-SO_3H$), (*ii*) carboxylic acid (-COOH), (*iii*) phosphonic acid ($-PO_3H_2$), and (*iv*) sulfonyl imide ($-SO_3NHSO_2CF_3$). The backbone along with any cross-links confers appropriate thermomechanical properties, inertness, and extent of swelling, while the number (equivalent weight, *EW*) and strength (p*K*) of acid groups confers the electrolyte properties.

The perfluorinated PEMs are the most commercially advanced membranes owing primarily to their chemical inertness.[5-8] Thus, Nafion has demonstrated fuel cell lifetimes of over 60,000 h at 80°C,[9] although higher temperature lifetime studies have not yet been reported. The polytetrafluoroethylene (PTFE) backbone enhances the chemical and mechanical properties of the PEM albeit at the cost of limited water sorption due to its hydrophobicity. Other perfluorinated membranes include the Dow membrane which has a shorter side chain than Nafion but otherwise has similar structural and morphological properties.[10] Both Aciplex-S and Flemion, available from Asahi Chemical and Asahi Glass Company, respectively, have long side chain perfluorosulfonated membranes with performance similar to Nafion. Perfluorinated PEMs have been developed by modification of the acid group.[11-13] Thus, DesMarteau[12,14] replaced the sulfonic acid group ($-SO_3H$) in Nafion with a sulfonyl imide group ($-SO_2NHSO_2CF_3$), which results in an increase in the water uptake while Kotov *et al.*[13] developed membranes with a phosphonic acid group that has the potential for higher thermal sta-

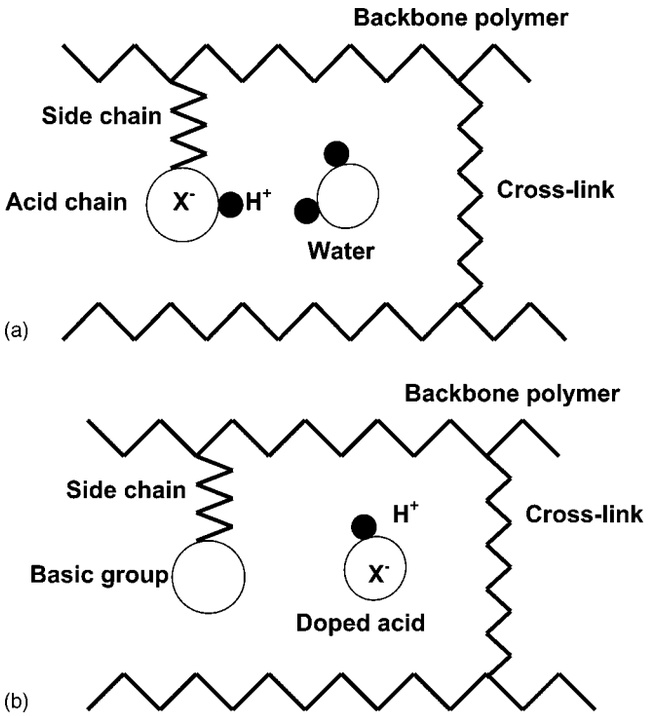

Figure 1. Schematic of structure of (a) PEMs and (b) PACs.

bility. Other perfluorinated PEMs include Gore-select[15] which uses a PTFE matrix embedded in the perfluorinated PEM to provide mechanical strength, thus allowing membrane thickness to be reduced to below 20 μm. These membranes possess conductivity up to 0.01-0.1 S/cm depending on RH.

Partially fluorinated PEMs such as the sulfonated trifluorostyrene membranes[16] have also been developed. Ballard Power Systems has developed BAM3G,[17] a family of PEMs with equivalent weights 375 to 920, by incorporating α,β,β-trifluorostyrene monomer, and a series of substituted α,β,β-trifluorostyrene comonomers. These membranes are less expensive than Nafion and have demonstrated good stability (>15,000 h).

The alternate hydrocarbon backbone-based polymers not only provide the potential for high-temperature performance at low RH, but also promise a cost advantage.[18,19] The early research with hydrocarbon PEMs was abandoned due to their short life spans. However, the new generation of polymers designed for higher temperature and corrosion resistance include sulfonated poly(oxy-1,4-phenyleneoxy-1,4-phenylenecarbonyl-1,4-pheneylene) or polyether ether ketone (PEEK), poly(4-benzoyl-1,4-phenylene) (PPBP), sulfonated poly(phenylene sulfide), alkylsulfonated polybenzimidazol (AS-PBI), and sulfoarylated PBI. Others include polyphosphazene (PP), polyether sulfones, polyphenylene oxide (PPO), poly(phenyl quinoaniline) (PPQ), polyimide, and styrene/ethylene-butadiene/styrene copolymer. McGrath and co-workers have presented promising MEA results utilizing poly-(arylene ether sulfone) PEMs.[20,21]

Polymer-acid complexes (PACs).—Figure 1b shows a schematic of the basic elements of a PAC including the backbone, cross-links, basic sites, and the doped acid electrolyte. PACs are distinct from PEMs in that the acid is not covalently bound to the polymer but is retained with the help of basic sites within the polymer. Thus, both anion and protons are mobile. A recent example of a PAC that has generated considerable interest is the H_3PO_4/PBI membrane.[22] PBI is basic ($pK_a \sim 5.5$) and forms a complex with H_3PO_4. The conductivity depends upon doping level. For 5 mol H_3PO_4/PBI unit, $\sigma > 10^{-4}$ S/cm at 25°C and $\sigma > 3 \times 10^{-2}$ S/cm at 190°C are achieved. However, the long-term stability of these needs to be carefully investigated. Other examples of PACs include poly(ethyleneimine) (PEI), poly (vinylpyrrolidone) (PVP), and poly(acrylamide) (PAAM).[3] The acids commonly used for doping are H_3PO_4, H_2SO_4, HCl, and $HClO_4$. Until the longetivity issues are clear, PACs are not considered suitable for developing composite polymer electrolytes.

PEMs with solvents of lower volatility.—The solvent, *e.g.*, water or methanol in the PEM works as a Bronsted base by solvating the protons of the pendant acid. A possible approach, therefore, for increasing the operating temperature of the PEM at low relative humidity is to replace water with a lower volatile solvent. Thus, Savinell *et al.*[23] utilized H_3PO_4-doped Nafion and were able to attain high conductivity at elevated temperatures. However, H_3PO_4 is corrosive and would eventually leach out with the liquid water produced. Similarly Doyle *et al.*[24] demonstrated that Nafion imbibed with ionic liquids such as the molten salt 1-butyl, 3-methyl imidazolium triflate (BMITf) provides good conductivity at high temperatures. Unfortunately, the challenge of complete immobilization of the ionic liquid must first be addressed to ensure stable cell performance over extended periods.

Composite proton-exchange membranes (CPEMs).—Malhotra and Datta[4] first proposed the incorporation of inorganic solid acids in the conventional polymeric ion-exchange membranes such as Nafion with the objective of serving the dual functions of improving water retention as well as providing additional acidic sites. Thus, they doped Nafion membranes with heteropolyacids, *e.g.*, phosphotungstic acid (PTA),[25] and were able to show high cell performance at low RH and elevated temperature (120°C). The improved performance was ascribed to the presence of PTA that provides high proton concentrations and improved water retention. Unfortunately, due to high water solubility, the PTA eventually leaches out from the PEM.[26] Recently, Fenton *et al.* have shown that Nafion-PTA membranes can be stabilized by heat-treatment and the leaching of PTA can be reduced.[27]

To decrease the humidification requirements of PEMs, Watanabe *et al.*[28-30] modified Nafion PEMs by the incorporation of nanosized particles of SiO_2, TiO_2, Pt, Pt-SiO_2, and Pt-TiO_2. These modified PEMs showed a much higher water uptake. When operated at 80°C under low humidification PEMFC, the modified PEMs showed lower resistance than Nafion. This improvement was attributed to the suppression of H_2 crossover by *in situ* Pt and to the subsequent sorption of the water produced on the incorporated oxides.

Based on the above two pioneering studies, there is now a great deal of effort along the lines of development of organic-inorganic composite membranes.[31-34] Thus, Adjemian *et al.*[35,36] introduced nanosized SiO_2 into Nafion pores[37] and tested various thickness and EW membranes. The benefit of these composite membranes appears to be stable operation *vs.* conventional Nafion at a cell temperature of 130°C due to high rigidity, both tested under fully humidified conditions. The investigators note that the unmodified PEMs showed thermal degradation, while the SiO_2-modified PEMs did not show such damage. Costamagna *et al.*[31] incorporated zirconium phosphate into a Nafion 115 membrane[38] and the results obtained are similar. Zaidi *et al.*[39] embedded heteropolyacids to different extents in sulfonated polyether ether ketone (S-PEEK). The highest performing composite was a tungstophosphoric acid doped, 80% sulfonated PEEK PEM. It showed conductivity similar to that of Nafion.

Inorganic acidic additives.—Although there exist numerous liquid superacids [*e.g.*, mixtures of HSO_3F and SbF_5, with Hammett acidity (H_0) = −20], which could enhance conductivity, they are unsuitable for fuel cell applications as it is a challenge to immobolize them within the PEM. Thus, solid acids are of the primary interest as additives. The heteropolyacids (HPA) are an example of a class worth investigating as they demonstrate high acidity and hy-

drophilicity. These properties could be exploited if HPAs could be anchored within the polymer matrix, *e.g.*, using cesium salts of HPAs.

The sulfated metal oxides, such as TiO_2, ZrO_2, and Fe_2O_3, have become subjects of intensive catalytic studies because these strong superacids are thermally more stable than other solid superacids.[40] Currently, sulfated zirconia (SO_4^{2-}/ZrO_2) is the strongest superacid among all known solids ($H_0 < -16$).[41] It retains the sulfonic acid groups, responsible for proton conduction, until about 500°C. As SO_4^{2-}/ZrO_2 exhibits the highest acidity of all the solid superacids,[42] the additives selected in the study are based on zirconia.

Systematic Design of Composites PEMs

It is evident from the literature that composite PEMs (CPEMs) are promising for higher temperatures above 120°C. However, the investigations done so far have not been systematic. Thus, a more systematic approach to the design of CPEMs is discussed here. As a start, let us first review the reasons for improvement of CPEMs.

Higher water retention in the CPEMs: the presence of a hygroscopic additive binds a larger amount of water in the membrane, increasing the membrane water content at a given RH.

Greater number of acid sites: this increases the concentration of mobile protons.

Lower gas crossover: the presence of nanoparticles in the membrane pores reduces the permeability of gas through the membrane. The crossover current measured with the modified membrane is an order of magnitude lower than that of the unmodified PEMs.

Improved thermomechanical properties: there are indications that the T_g and Young's Modulus of the polymer are improved by incorporation of inorganic additives.

Improved electrode performance: due to the increased water retention in the modified PEM, an extended reaction zone maybe available,[43] resulting in better electrode performance at high temperatures.

The reasoning above is, however, qualitative. In order to better appreciate some of the key factors involved in the design of a high-temperature composite Nafion-based PEM, it is beneficial to consider this within a framework of a quantitative model of the conductivity. Such a model is readily obtained by an extension of our previous work on simulation of the transport of protons through a Nafion membrane at different temperatures and RHs.[44] This transport model is based on the dusty-fluid model (DFM),[45] where the obstruction presented by the polymer matrix to proton diffusion is viewed as an additional frictional interaction with large immobile dust or gel particles. Within this framework, the inorganic additive is simply viewed (Fig. 2) as an additional dust species immobilized within the polymer matrix.

The final form that describes the proton conductivity of a composite PEM is

$$\sigma = (\varepsilon - \varepsilon_0)^q \left(\frac{\lambda_{H^+}}{1 + \delta_{AH} + \delta_{ZH}} \right) (c_{AH,0}\alpha_{AH} + c_{ZH,0}\alpha_{ZH}) \quad [1]$$

with $\delta_{AH} = D_{12}/D_{1M}$ and $\delta_{ZH} = D_{12}/D_{1Z}$. Here D_{12}, D_{1M}, and D_{1Z} are the diffusion coefficients for (H_3O^+)/solvent (H_2O), H_3O^+/PEM matrix and H_3O^+/additive particle, respectively. In Eq. 1, ε and ε_0 are the volume fraction of water in the membrane and the percolation threshold, respectively, where ε is a function of the water uptake (λ_{H_2O})

$$\varepsilon = \frac{\lambda_{H_2O}}{\frac{\overline{V}_M}{V_{H_2O}} + \lambda_{H_2O}} \quad [2]$$

where $\overline{V}_M$ is the effective partial molar volume of the PEM and is calculated as

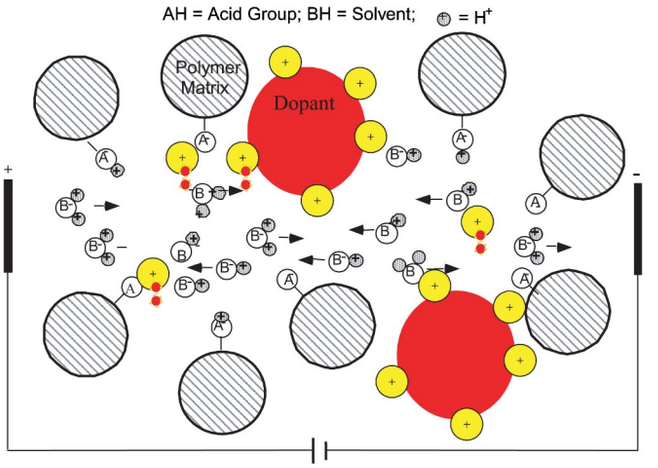

Figure 2. A dusty-fluid model depiction of a PEM describing proton conductivity through the Nafion polymer matrix and the superacidic dopant. The framework treats the Nafion matrix as large dust particles through which the current carrying ions must traverse.

$$\overline{V}_M = \overline{V}_{PEM}(1 - \omega_Z) + \overline{V}_Z\omega_Z \quad [3]$$

where the partial molar volume of the additive, $\overline{V}_Z = d_Z/(6c^*_{ZH_0})$, where $c^*_{ZH_0}$ is the surface acid site density of the additive (mol/cm^2) and d_Z is the additive particle size. Also ω_Z is the mass fraction of the additive in the composite PEM. ε_0 is defined in a similar manner, being based on the water uptake at monolayer coverage.[44] The Bruggeman, or critical, exponent $q = 1.5$, and λ_{H^+} is the equivalent conductance of a proton in water. The solvent uptake in the transport model can be predicted by either the finite layer Brunauer-Emmett-Teller (BET) isotherm of Thampan *et al.*[44] or by the more sophisticated approach recently developed by Choi and Datta.[46] Thus at low RH, the water uptake of the PEM is low and the resulting low ε results in poor conductivity. The water uptake and the conductivity rise sharply above ~70% RH.

The concentration of acid sites available within the PEM is the sum of the pendant acid sites $c_{AH,0}$ in the polymer plus the additive acid sites, $c_{ZH,0}$. Of course, these sites only contribute to the conductivity when the protons are dissociated in the presence of water or other solvent. The extent of dissociation depends upon the level of hydration and the strength of the acid groups, and is denoted as α_{AH} and α_{ZH} for the polymer and the additive, respectively.[44]

Thus, within the framework of this simple model for the design of composite PEMs, the objective of increased PEM conductivity at lower RH and higher temperature may be achieved by the presence of hygroscopic acidic additives, since:

The presence of a hydrophilic additive increases the water uptake ε or λ_{H_2O} of the PEM at a given RH, as shown schematically in Fig. 3. In other words, the equilibrium content of water in the membrane is shifted to higher values at a given vapor activity, because of greater number of acid sites and since water is bound more strongly. However, the Young's modulus E of the polymer also increases with the additive, which counters the increased hydrophilicity and hence also affects swelling.[44]

The presence of the acid sites on the surface of nanoparticles increases the total number of acid sites available within the PEM as shown in Fig. 2, effectively reducing $\overline{V}_M$ (Eq. 3). This enhances the conductivity because the number of charge carriers available increases correspondingly (Eq. 1).

The number of additional acid sites is proportional to the specific surface area of inorganic particles, $S_Z = 6/(\rho_Z d_Z)$ (cm^2/g), where

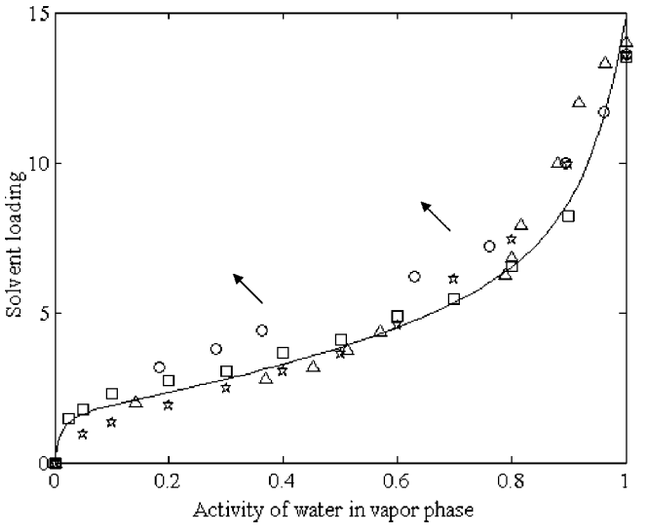

Figure 3. The solvent loading *vs.* activity of water vapor for Nafion (EW = 1100) membrane (triangle: Ref. 20, square: Ref. 21, circle: Ref. 44, and star: This work). The design objective is to increase the solvent loading of Nafion. The composite will adsorb more water at fixed RH *vs.* unmodified Nafion resulting in higher conductivity at low RH.

d_Z is the additive particle size and ρ_z is its density. Thus, smaller particles are better for a given loading.

There is an optimum amount of additive loading ω_Z in the PEM. This is so since the diffusional resistance represented by δ_{ZH} would increase with loading as more nanoparticles occupy the pore volume. Also from Eq. 3 we understand that $\overline{V}_M$ would first decrease and then increase depending on $\overline{V}_Z$.

Additionally, the additive must be selected in a way (*i*) such that it can be immobilized within the polymer matrix, (*ii*) which is compatible with the electrocatalyst, and (*iii*) which can maintain/increase the thermomechanical properties of the polymer at higher temperatures. Thus materials that may leach out or poison the membrane or electrocatalyst are not useful. Another factor affecting performance is that, since the acid dissociation constants decline with temperature, the degree of dissociation and hence the number of charge carriers decline at higher temperatures.[44] It must also be noted that the particle size of the additive particles (dust) is crucial both because they form an additional diffusional barrier to the transport of protons (Eq. 1), and because the number of surface acid sites depend upon the particle surface area.

Experimental

The experimental methods involved additive synthesis, composite membrane fabrication, and additive and PEM characterization via water uptake and *ex situ* conductivity measurements.

Composite PEM synthesis.—Composite membranes were fabricated by two alternate methods: (*i*) mixing Nafion gel and inorganic particles followed by membrane casting, and (*ii*) *in situ* nanoparticles synthesis via sol-gel processing in precast or commercial Nafion membranes.

The first procedure was utilized so that the literature protocol of producing sulfated zirconia (requiring calcination at 600°C) could be followed for producing the particles first. However, this procedure resulted in relatively large particles (in the micrometer range). The second procedure was followed to produce nanoparticles *in situ* using the precast Nafion as a template. However, particles formed by this procedure were evidently not amenable to the high-temperature sulfation procedure.

Zirconia particle preparation.—The SO_4^{2-}/ZrO_2 particles were synthesized based on Arata's work on metal oxides.[47] Thus, ZrOH powder (MEI Chemicals, Flemington, NJ) was stirred in 0.5 M H_2SO_4 for 15 min at room temperature. The acid was decanted, and the remaining powder dried at 100°C overnight. The dried powder was then calcined in air at 600°C for 2 h and the resulting particles were crushed with a mortar and pestle. These particles are denoted here as SO_4/ZrO_2.

Particles were also prepared from a colloidal solution of 20 wt % ZrO_2/acetic acid (Nyacol Nano. Technologies, Ashland, MA). The solution was evaporated and the ZrO_2 precipitate was obtained. This precipitate is denoted as ZrO_2. The precipitate was heated in 6 M H_2SO_4, in order to sulfate the ZrO_2, then dried at 120°C for 2 h, and finally calcined in air at 600°C for an additional 2 h. The resulting particles were crushed with a mortar and pestle, and are denoted as ZrO_2 (A). Additionally, a sample of the ZrO_2 (A) was pulverized with a Jet Mill (Laboratory Jet Mill, Clifton NJ) to obtain a reduction in the particle size. This sample is denoted in the following as ZrO_2 (AP).

Cast composite membranes.—Based on experimental procedures described in the literature,[48] the protocol described below was developed to produce uniform and reproducible cast PEMs. To obtain the desired weight loading of additive Ω_Z in the PEM, selected additive particles were dispersed in a 23 wt % Nafion/ethanol solution with a magnetic stirrer. After stirring for 8 h, the solution was cast as a PEM on a glass dish utilizing a doctor blade. The cast membrane was placed in a convection oven at 100°C for 15 min, which was sufficient to produce a solid membrane. The PEM was removed from the glass dish with DI water, dried, and then annealed in a Teflon sleeve at 170°C at 10 tons for 15 min in a mechanical press (Carver model C, Wabash, IN). This processing step was necessary to produce pliant, insoluble PEMs with mechanical properties similar to those of commercially available Nafion films. The resulting cast PEM had a thickness of around 50 μm.

Sol-gel ZrO2—Nafion, composite PEMs.—The alternate method of preparation of a ZrO_2 composite PEM was via *in situ* sol-gel synthesis based on methods developed by Mauritz's and co-workers for the synthesis of asymmetric ZrO_2/Nafion composites.[49] In this procedure, the host PEM serves as a template that directs the morphology and particle size of the oxide in the PEM matrix, resulting in nanosized particles.[50] As received Nafion membranes (Sigma-Aldrich Corp., St. Louis, MO) were boiled in 3 wt % H_2O_2 for 1 h and then rinsed in water. They were then immersed in 50% vol HNO_3/H_2O and heated for 6 h, rinsed in water, and then heated in 50% vol H_2SO_4/H_2O for an additional 6 h. The membranes were finally boiled in water for 1 h and then rinsed and washed in water several times to ensure complete removal of any residual acid.

The purified membranes were then placed in a vacuum oven and heat-treated at 110°C for 12 h. Thereafter, the membranes were boiled in H_2O for 1 h and subsequently dried at 50°C for 4 h. The membranes were then immersed in 10:1 ethanol/H_2O solution for an additional hour. The ethanol/H_2O mixture served to further swell the pores of the PEM to maximize the absorption of the precursor solution. The membrane was removed and immersed into a 20:1 (v/v) ethanol: zirconium tert-butoxide solution for 10 min and then rinsed in ethanol in order to remove surface ZrO_2. The membranes were then removed and heated at 110°C in vacuum for 24 h to complete the condensation reactions. This composite PEM is denoted here as Nafion ZrO_2 sol-gel.

The membranes synthesized by this method are completely transparent and homogenous as compared to membranes prepared by the casting method which were cloudy due to the much larger particles. Figure 4 shows SEM (Amray model 1610 Turbo SEM) images for both the membranes. The membrane prepared using the casting method had larger zirconia particles with size ranging in 5-15 μm. On the other hand, the sol-gel membranes showed no X-ray scatter-

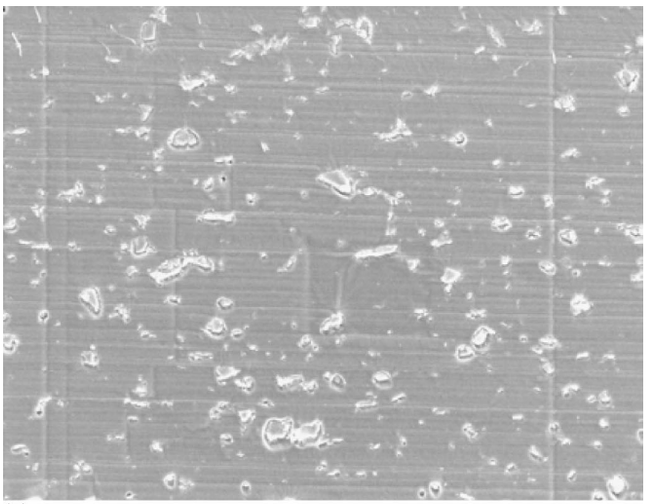
(a)

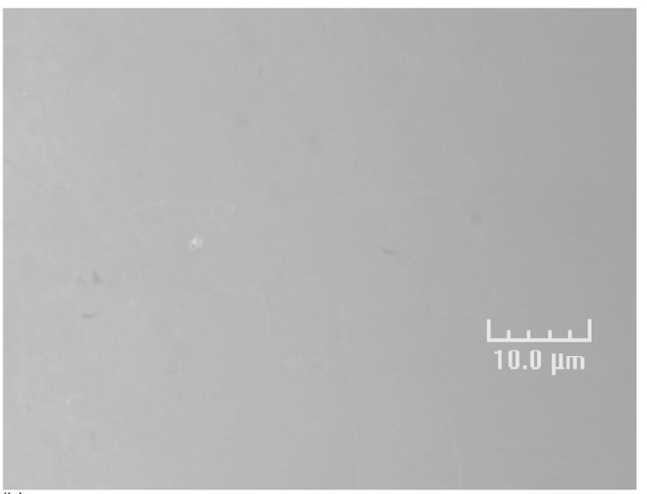

(b)

Figure 4. SEM images of membranes synthesized by both the *in situ* and doping methods. (a) Nafion ZrO_2 doped membrane. (b) The Nafion ZrO_2 sol-gel PEM is homogeneous and transparent demonstrating no phase separation.

ing. Also the surface of sol-gel membranes did not show any deposition of oxides which confirms that the zirconia is present within the pores of the Nafion membrane. This provides evidence that these membranes have nanosized zirconia particles within the pores of the membrane.

Composite membrane characterization.—Water uptake measurements.—To measure the water uptake of the composite PEMs, a tapered element oscillating microbalance (TEOM series 1500 PMA reaction kinetics analyzer, Rupprecht & Patashnick, Co., Inc., Albany, NY) was utilized.[51] The sample mass change in TEOM is measured as the frequency change in the tapered element oscillation. The instrument has a sensitivity of 1 μg and a temperature range of up to 700°C. The RH was controlled by mixing metered flows of a wet (saturated with H_2O) and a dry helium stream. Calibration was done with a RH meter (FH A646-R, ALMEMO, Ahlborn, Munich, Germany). The membrane was cut into thin strips (1.5 by 1.5 mm) and packed carefully along with quartz wool into the oscillating glass chamber of the TEOM to avoid rattling. The water uptake was measured for all samples at 25 and 90°C from 0 to 90% RH, and at 120°C from 0 to 40% RH. After the sample was loaded, it was exposed to the helium gas with the desired RH, and the real-time mass change was observed to determine when the equilibrium amount of water had been adsorbed onto the membrane.

Ion-exchange capacity measurements[52].—A 0.2 g sample of the composite PEM was exchanged with NH_4^+ by immersing the sample in 1 M ammonium acetate for 24 h and then in ammonium chloride for an additional hour. The PEM was then washed with DI water to remove any excess NH_4^+ ions. To ensure that all excess NH_4^+ had been removed, a drop of 1 M silver nitrate was added to the wash. If NH_4^+ ions were present, a white precipitate would form. The PEM was then stored in 50 mL DI water. Adding 2 mL of 5 M NaOH solution to the sample, caused the subsequent exchange of NH_4^+ with Na^+. Utilizing a calibrated ammonia electrode (model 95-12 Orion, Boston, MA), the amount of NH_4^+ released could be accurately quantified thus providing a measure of the ion-exchange capacity.

Ex situ conductivity testing.—A composite membrane sample was sandwiched between two electrodes each on either side to measure the conductivity, similar to the procedure reported in literature[53] and then placed in a humidity-controlled chamber. The humidity of the chamber was monitored utilizing a dewpoint/temperature probe (HMP 238, Vaisala, Woburn, MA). An air stream was saturated with water by bubbling through a humidifier. This wet stream was heat-traced to the chamber to avoid condensation. The chamber and the humidifier were both heated to 90 and 120°C, respectively, to obtain the desired partial pressure of water. The conductivity of the PEM was measured at 90°C in the RH range from 10 to 90%, while at 120°C the RH range was from 10 to 40% to simulate dry conditions. These conditions are the same as those utilized for the water uptake measurements. The conductivity measurements were made with a perturbation voltage of 10 mV in the frequency range 0.01 Hz to 10^6 Hz using a Solartron SI 1260 FRA (Solartron, Hampshire, UK). Both real and imaginary components of the impedance were measured and the real *z* axis intercept was closely approximated to provide an estimate of the membrane resistance, and hence, conductivity.[55]

MEA testing.—The electrodes utilized are commercially available from E-TEK (Somerset, NJ). The type selected was the single-sided ELAT® gas-diffusion electrode (20% Pt-on-C, 0.35-0.4 mg Pt/cm^2). The active layer of electrode was brushed with 5% Nafion solution (0.6-0.8 mg/cm^2 MEA). This electrode was placed on either side of the PEM and the resulting membrane-electrode assembly (MEA) placed in a hot press. The temperature of the hot press was then raised to 130°C and a pressure of 272 atm applied for 120 s. The MEA thus prepared was mounted in a 5 cm^2 fuel cell test fixture, obtained from Fuel Cell Technologies (Los Alamos, NM). The cell was fed with humidified H_2 and O_2 or air supplied at pressure 1 to 3 atm utilizing electronic mass flow controllers (MKS model no. 1179A22CS1BV-S, Andover, MA) and was controlled by the electronic load (Series 890B Fuel Cell Test System, Scribner Associates, Inc., Southern Pines, NC). Utilizing software (Fuel Cell Test Software Version 2.0, Scribner Associates, Inc.), the mass flow rate of the feed gas was programmed to stoichiometry-dependent flow rates. The load has an inbuilt feature of measuring *in situ* MEA ohmic resistance utilizing the current interruption method.

The pressure of the reactant gases was monitored using pressure gauges (Matheson, model no. 63-5612). Back-pressure regulators (Tescom model no. 44-2300) were used at the outlet of both the anode and the cathode to control the gas pressure. Humidification of the cell was accomplished by bubbling the feeds through stainless steel cylinders containing DI water and equipped with a sight glass. Heating tape was wrapped around the feed lines to prevent any condensation in the lines, and water traps were added after the exit gas stream to facilitate removal of water. The temperature of the humidifiers as well as that of the fuel cell was controlled using individual temperature controllers (Omega CN9100A).

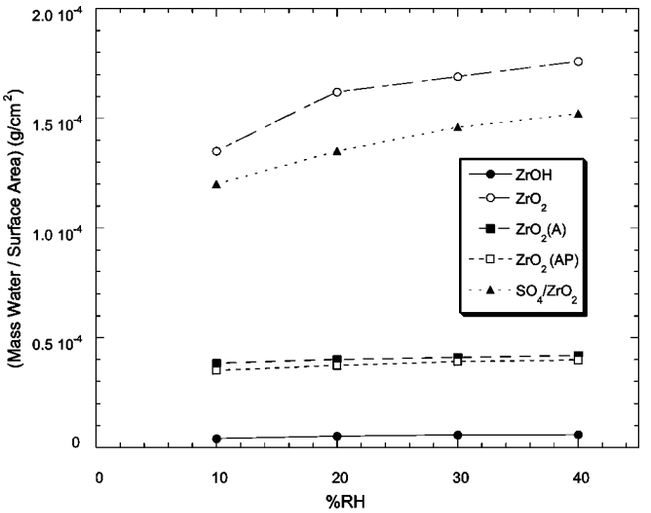

Figure 5. The surface area normalized water uptake of the powder at 120°C *vs.* RH. The most promising candidates are the ZrO_2 and the SO_4/ZrO_2 samples.

The following MEA test protocol was utilized.[54] The start-up procedure involved bringing the humidifier temperature up to a set value of 80°C, then increasing the fuel cell to 70°C and operating with 1 atm H_2 and air at current controlled mass flow rates, being 1.3 times anode stoichiometric flow for H_2 and 2.0 times cathode stoichiometric flow for air. The load was cycled for an additional 6 h and then a constant voltage polarization curve was taken. Thereupon, another 12 h of break-in period was utilized and then a final polarization curve was obtained as follows. The voltage was set at 0.6 V set for 10 min then data was taken every 6 s for 3 min. The voltage was held for 3 min, before the first data point was collected, and then data were collected every 6 s for 3 min at each voltage set point. This continued for the following voltage sequence, 0.55, 0.5, 0.45, 0.4, and 0.6 V, 1 (for 1 min), 0.65, 0.7, 0.75, 0.8, 0.85, and 0.6 V.

The electrochemical surface area (ECSA) and crossover were measured utilizing the potentiostat. Potentiostats often allow the choice of two, three, or four terminal connections to the cell depending on the particular application to measure the ECSA and crossover current. The two terminal connections are usually used when it is difficult to position the reference electrodes inside the cell itself. Although there is a reference electrode machined in the test fixture, it is assumed that the H_2 anode behaves as a reference electrode. The ECSA is a measure of the surface area of Pt that takes part in the reaction and was measured in the following manner: (*i*) The cathode was purged with N_2 and the anode with H_2, both set at 50 sccm and 1 atm. (*ii*) After the open circuit voltage (OCV) is <0.14 V, the ECSA was measured by utilizing the 1287 potentiostat (Solartron, Hampshire, UK). The counter electrode (CE) and reference electrode 1 (RE 1) were connected to the anode, while the working electrode (WE) and the reference electrode 2 (RE 2) were connected to the cathode. (*iii*) To measure the ECSA of the MEA, the potential was swept from 0.0 to 0.6 V for four cycles at 100 mV/s, while the crossover was measured at 0.0 to 1.0 V at 2 mV/s for three cycles. (*iv*) The total charge between 0.0 and 0.6 V was integrated and after correcting for the double layer (assuming it is the baseline), the total charge produced by the reaction was calculated. The ECSA was calculated by assuming a stoichiometry of 1 e^-/Pt site.[55] The crossover is simply the plateau in current observed.

The pressure of the cell was next increased to 1.5 atm for both the H_2 and air feeds, and a polarization curve was obtained again. The temperatures of the fuel cell and the humidifiers were then increased to 80°C. After utilizing the break-in protocol for 2 h, to ensure that a steady-state performance has been reached, a polarization curve was obtained. Finally, the ECSA and crossover current were measured again.

In a similar fashion, the polarization curves and ECSA were measured at increasingly higher temperatures. The temperatures of the humidifiers were maintained at 80°C and the cell temperature

Table I. The partial molar volume, experimental, and predicted EW of the Nafion 112, and composite membranes at 25°C.

Samples	Partial molar volume $\overline{V}_M$ (cm^3/mol)	EW (g/mol. H^+) (experimental)	EW (g/mol. H^+) (from Eq. 3)
Nafion 112	537	1106	1106
Nafion ZrO_2 sol-gel.	515	1016	1030
5% ZrO_2 (A)	517	1084	1084
10% ZrO_2 (A)	528	1121	1109
20% ZrO_2 (A)	545	1159	1146

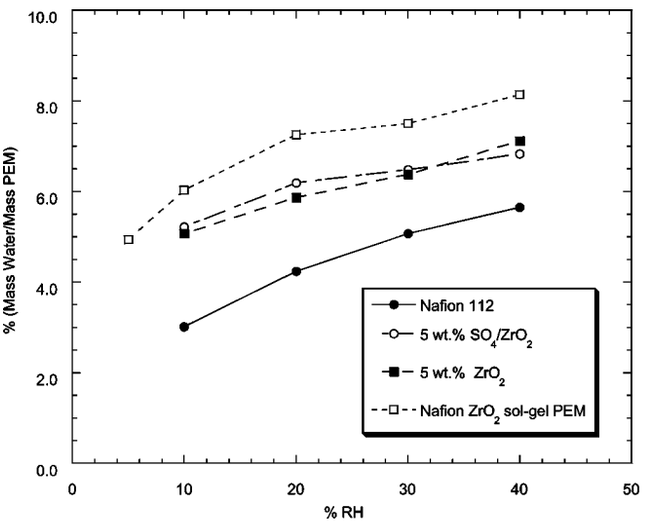

Figure 6. The water uptake of composite membranes and Nafion 112 at 120°C *vs.* RH. The Nafion ZrO_2 sol-gel PEM demonstrates the highest water uptake.

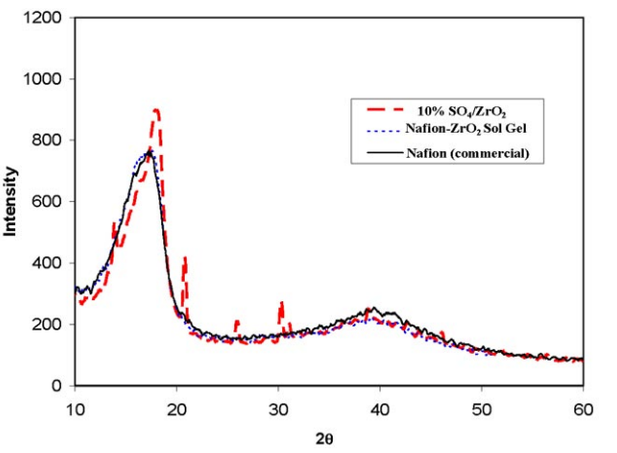

Figure 7. XRD pattern for composite membranes and Nafion.

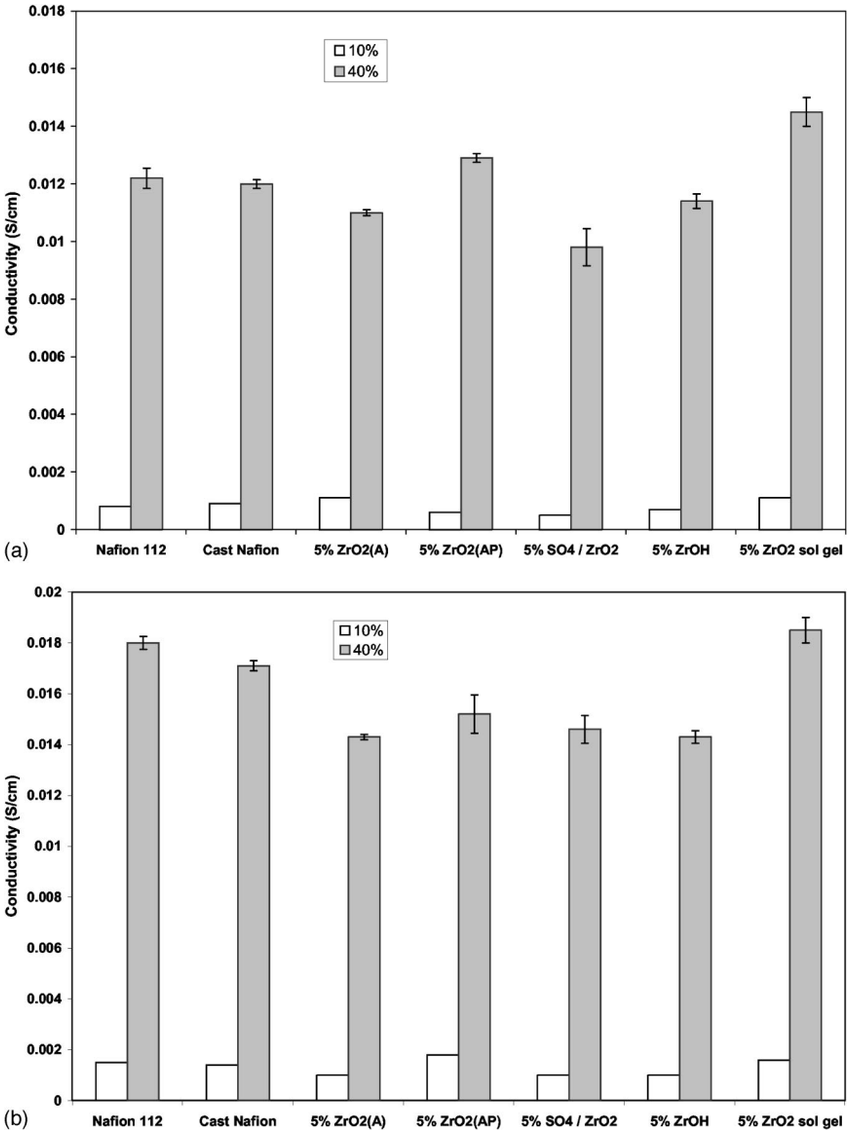

Figure 8. (a, top) The conductivity of the PEMs at 10% RH and 40% RH at 90°C. The Nafion ZrO_2 sol-gel PEM shows the highest conductivity of the samples. (b, bottom) The conductivity of the PEMs at 10 and 40% RH at 120°C. The Nafion ZrO_2 sol-gel PEM shows the highest conductivity of the samples.

was returned to 70°C at the end of the experiment. Thus, the sequential temperature test protocol was: (*i*) cell = 70°C, hum. = 80°C, beginning of life (BOL), (*ii*) cell = 90°C, hum. = 80°C, (*iii*) cell = 100°C, hum. = 80°C, (*iv*) cell = 110°C, hum. = 80°C, (*v*) cell = 120°C, hum. = 80°C (*vi*) cell = 130°C, hum. = 130°C, $P = 3$ atm O_2, and (*vii*) cell = 70°C, hum. = 80°C, end of life (EOL).

Results and Discussion

Water uptake measurements.—Figure 5 shows the area specific water uptake at 120°C of all the additive powders utilized in this study. Among the additives investigated the most promising appears to be the ZrO_2 (sample with no acid treatment). Figure 6 shows the water uptake of the composite membranes measured at 120°C. All the composites show an enhanced water uptake at 120°C when compared to Nafion. The Nafion ZrO_2 sol-gel composite shows the highest water uptake of all the samples tested and is around 40% higher than Nafion 112 at 40% RH. The 5 wt % SO_4/ZrO_2 and the 5 wt % ZrO_2 both show water uptake that is 20% higher than the Nafion 112 sample at 40% RH. Thus, the behavior of the composite PEMs reflects the trend due to the effect of size of inorganics particles. The Nafion ZrO_2 sol-gel composite has the smallest particle size as compared to other membranes and hence, has the highest water uptake of all the composites. Further, the benefit of inorganic additives in PEMs is evident at higher temperatures and low RHs.

Ion-exchange capacity.—Table I lists the experimental EW and partial molar volumes along with the predicted EW using Eq. 3 for the composite membranes. The additive acid site concentration c^*_{ZH0} was estimated using data for 5% ZrO_2 (A) EW and assuming an average 10 μm particle size as 7.77×10^{17} molecule/cm^2. Assuming c^*_{ZH0} constant for all the composite membranes, the partial molar volume of other composite membrane was calculated and is listed in Table I. The corresponding EW can be thus obtained by multiplying V_M with the measured membrane density. The EW obtained from Eq. 3 and experimentally are in good agreement. Thus, it is evident that for nanosized particles, the EW is low, implying higher acidity. Also it is observed that an increase in particle size increases the V_M which causes a decrease in the acidity of the membrane. The Nafion ZrO_2 sol-gel composite has the highest number of acid sites available of the membranes investigated due to the larger surface area of the nanosized particles. Based on gravimetric and preliminary ash analysis, the loading of particles in the Nafion ZrO_2 sol-gel composite is around 3 to 4 wt %. The incorporation of zirconium oxide in

Nafion using the sol-gel method increased the effective acid site concentrations in the membrane also resulting in higher water uptake.

The X-ray diffraction (XRD, model Rigaku Geigerflex X-ray diffractometer) analysis for the composite membranes compared to Nafion shown in Fig. 7 was done at room temperature. The 10 wt % SO_4^{2-}/ZrO_2 showed some extra peaks as compared to Nafion corresponding to ZrO_2. However, the Nafion ZrO_2 sol-gel showed a pattern essentially identical to Nafion due to the low loading and the nanosized ZrO_2. Hence a future goal is to increase the loading of ZrO_2 in the membrane by varying the synthesis procedure during the sol-gel process.

It is evident that for the membrane to be more acidic, the equivalent weight ought to decrease. However, lowering the EW implies that the membrane would swell more due to high water sorption. However, the mechanical strength of the membrane is also related to the additive loading. Thus, an optimum amount of inorganic additive is indicated. Polymeric membranes with an EW below 900 show low mechanical strength and are not suitable for fuel cell applications. Hence an objective is to design membrane having EW around 900 for best fuel cell performance with the highest water uptake and proton conductivity.

Conductivity measurements.—Figure 8a shows the measured conductivity of the commercial Nafion 112, solvent cast Nafion, and the solvent cast and the sol-gel composite PEMs measured at 10% RH and 40% RH at a temperature of 90°C. The Nafion ZrO_2 sol-gel composite has the highest conductivity among all composites. Figure 8b presents the conductivity of the composite PEMs measured at 120°C. The conductivities for Nafion and other composite membranes were reproduced, and the error bars are shown for each composite. In general the conductivities at 120°C are higher than 90°C. The conductivity exhibited by the Nafion ZrO_2 sol-gel composite is about 4-5% higher than Nafion 112 at 40% RH. All the other composites have conductivities smaller than that of Nafion despite a higher water uptake.

The increase in the conductivity of the Nafion ZrO_2 sol-gel composite than that of Nafion is the combined result of the enhanced water uptake as well as acidity. Also the membrane structure influences the overall conductivity of the membrane. Our concomitant efforts to develop a proton transport model for both Nafion and CPEMs shows that tortuosity of the membranes affects the water sorption properties which in turn impacts the conductivity.[56] Although the other composites show an enhanced water uptake at 120°C, the acidity (Table I) as well as conductivity of these PEMs is less than that of Nafion. It is thus noteworthy that an enhancement in the water sorption properties of the PEM does not necessarily translate directly into an enhanced conductivity.[57]

To study the effect of the additive loading, the conductivity of 5, 10, and 20% ZrO_2 composites *vs.* RH is shown in Fig. 9a and b at 90 and 120°C, respectively. It is observed that the optimum conductivity in both cases is with the 10% ZrO_2 PEM. An increase in conductivity is observed when the loading is increased from 5 to 10%, while a dramatic decline is observed when the loading is increased a further 20%. Although the water uptake of the composites increases monotonically with loading of the additive, the IEC measurements show that an increase in the loading causes the EW to increase (Table I) and thereby reducing the acid strength of the composite membrane. Hence, enhanced water sorption with lower EW of the composite membrane and optimum loading will result in the highest conductivity.

MEA performance.—Figure 10 shows the fuel cell performance obtained with a Nafion 112 MEA that was tested at 70, 90, 100, 110, 120, 130°C and then returned to 70°C, following the test protocol described above. The performance drops with increasing temperature and a reduction in RH. To distinguish between the membrane resistance and the kinetics, the electrochemical surface area measurements were also made and are shown in Table II. As the temperature increases, the ECSA decreases due to ionomer shrinkage within the catalyst layer indicating a reduced active area, thus countering the increased rate of reaction at higher temperatures. For instance, when the temperature is increased from 90 to 120°C, the ECSA declines to one-third its value at 90°C. Kanamura *et al.*[43] investigated the Nafion/Pt interface with *in situ* spectroscopic techniques (Fourier transform infrared spectroscopy, atomic-force microscopy, and surface potential measurements). The interface was observed to have a dynamic nature, in the dry state the interface is very small while in the humidified state the interface was greatly extended. Additionally, the conductivity of the Nafion ionomer present within the catalyst layer will also drop at higher temperatures and low RH. Thus, the performance of the fuel cell is limited at lower RH at higher temperatures both due to the increased transport resistance in the PEM layer as well as due to the decrease in ECSA in the catalyst layer.

From Fig. 10 it is also observed that there is a decline in the performance not only as the cell temperature increases (and concomitantly as the RH decreases), but also between BOL and EOL polarization, of about 300 mA/cm^2 at 0.6 V. It is also noted that the ECSA measurements at 70°C BOL and 70°C EOL are 40.8 and 29.2 mC/cm^2, respectively, while the cell resistance measurements are

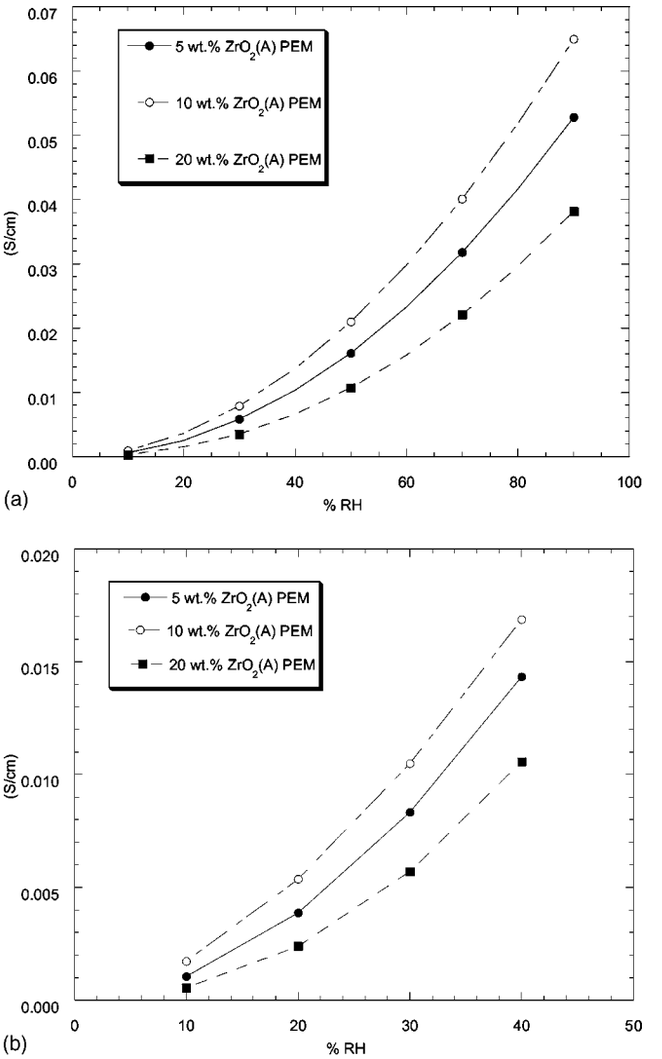

Figure 9. (a, top) The conductivity of loaded composites PEMs at 90°C *vs.* RH. The optimum conductivity is observed with the 10 wt % PEM. (b, bottom) The conductivity of loaded composite PEMs at 120°C. The optimum conductivity is observed with the 10 wt % PEM.

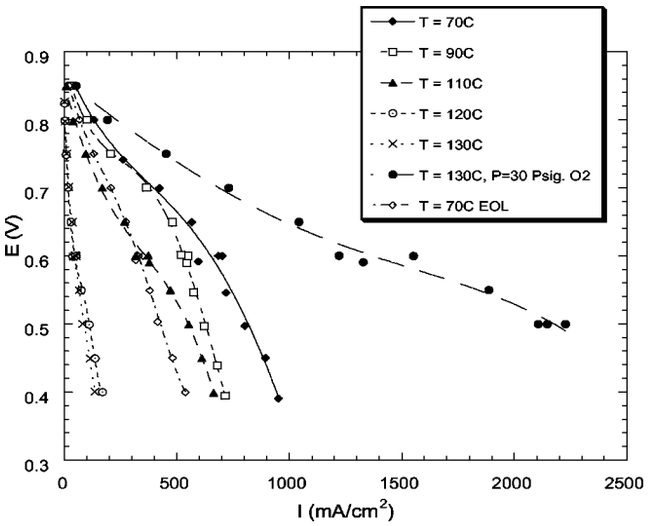

Figure 10. The cell performance of Nafion 112 MEA with conditions as noted on figure. Operated with 1.5 atm air/H_2, humidifiers set at 80°C. The exception was when the cell was at 130°C, 3 atm. O_2 and the humidifiers set at 130°C.

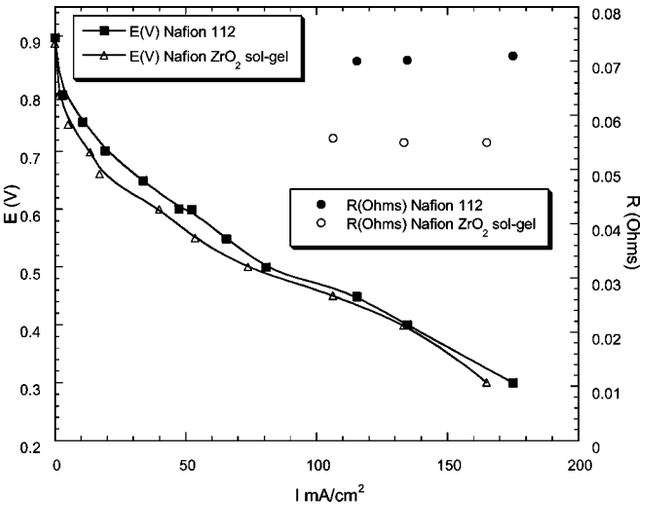

Figure 11. The cell performance of Nafion 112 MEA *vs.* Nafion ZrO_2 sol-gel composite MEA. Air and H_2 at 2.0 and 1.3 times stoichiometry flows, respectively, $P = 1.0$ atm., $T_{HUMIDIFIER} = 80°C$, $T_{CELL} = 110°C$.

20.3 and 21.5 mΩ at 70°C BOL and 70°C EOL, respectively. Thus, the performance loss is mainly a result of kinetic overpotential, as the ohmic PEM resistance measured at the BOL and EOL is similar. The crossover current measurements demonstrated low current (0.5 mA/cm^2) generated by H_2 crossover at high temperature (120°C). The excellent performance at 130°C under fully humidified conditions (humidifiers at 130°C, $P = 3$ atm) shows no degradation over several hours.

Finally, a MEA was fabricated with a Nafion/ZrO_2 sol-gel composite membrane and tested under dry hot conditions ($T_{cell} = 110°C$, $T_{Humidifier} = 80°C$). The resulting performance is shown in Fig. 11 along with Nafion 112 for comparison. Although no performance improvement was observed, it is noted that the *in situ* MEA ohmic measurements show improvement of conductivity of the composite *vs.* Nafion 112, under these conditions. However, it is clear that the reduction of ECSA in the catalyst layer under dry conditions (Table II) must also be addressed before improved performance can be obtained. It is noteworthy that the literature contains few results of improved MEA performance despite improved *ex situ* conductivity reported for some composite membranes.

Based on our earlier fuel cell model[58] simulations, an order of magnitude drop in conductivity from 0.05 S/cm at 80°C to 0.005 S/cm at 120°C with Nafion 112 under dry conditions is the cause of the poor cell performance. The most promising composite, Nafion/ZrO_2 sol-gel composite on the other hand, demonstrates enhanced conductivity and water sorption compared to Nafion 112. An important outcome from utilizing the sol-gel approach is that the composite membranes synthesized were homogenous. This implies that this approach can be used to synthesize homogeneous membranes with inorganics exhibiting higher acidity and better properties than Nafion. Therefore, it is evident that we need to further increase the conductivity of the composite PEMs for a substantial improvement in MEA performance at higher temperatures and low RH. Additionally, at lower RH and higher temperatures, the shrinkage and dehydration of the ionomer in the catalyst layer must also be addressed.

Table II. The ECSA of a Nafion 112 MEA at different fuel cell temperatures, when the temperature of the humidifers remains constant at 80°C.

Nafion 112 (°C)	ECSA (mC/cm^2)
70 (BOL)	40.8
90	43.8
110	21
120	15
70 (EOL)	29.2

Conclusions

Based on a systematic approach, the synthesis and *ex situ* and *in situ* performance of composite PEMs for higher temperature/lower RH operation have been investigated. The promising potential of the sol-gel composite PEMs has been demonstrated with improved hydration as well as conductivity at higher temperature and lower RH conditions. Although greater conductivity improvement is necessary to obtain high performance at higher temperatures/lower RH, the increase in rates of reactions, improved CO tolerance[59] and water management may provide useful power densities even with a smaller enhancement, provided that the shrinking of ECSA under dry conditions can be first addressed. Thus, the incorporation of the zirconia additives in the catalyst layer to minimize electrode overpotential, and the long-term evaluation of these MEAs by fuel cell testing is being undertaken. In summary, significant progress has been made in the understanding and design of composite PEMs, and it is expected that continued development following a systematic approach will eventually result in high performance composite PEMs.

Worcester Polytechnic Institute assisted in meeting the publication costs of this article.

References

1. P. Murugaraj, K. D. Kreuer, T. He, T. Schober, and J. Maier, *Solid State Ionics*, **98**, 1 (1997).
2. T. Norby, *Solid State Ionics*, **125**, 1 (1999).
3. P. Colomban, *Proton Conductors*, Cambridge University Press, Cambridge (1992).
4. S. Malhotra and R. Datta, *J. Electrochem. Soc.*, **144**, L23 (1997).
5. A. Eisenberg and J. S. Kim, *Introduction to Ionomers*, John Wiley & Sons, New York (1998).
6. S. C. Yeo and A. Eisenberg, *J. Appl. Polym. Sci.*, **21**, 875 (1977).
7. R. M. Ikeda, *Polymer Prepr. Am. Chem. Soc., Div. Polym. Chem.*, , 215 (1978).
8. H. L. Yeager and A. Steck, *J. Electrochem. Soc.*, **128**, 1880 (1981).
9. A. Steck, in *Proceedings of the 1st International Symposium on New Materials for Fuel Cell Systems*, O. Savagodo, P. R. Roberge, and T. N. Veziroglu, Editors, Montreal, Quebec, Canada, July 9-13, 1995, 74 (1995).
10. D. S. Watkins, in *Proceedings of 33rd International Power Sources Symposium*, Cherry Hill, NJ, June 13-16, 1988, The Electrochemical Society, Inc., p. 782 (1988).
11. M. Hogarth and X. Glipa, *High Temperature Membranes For Solid Polymer Fuel Cells*, ETSU F/02/00189/REP DTI/Pub URN 01/893 (2001).

12. D. D. DesMarteau, *J. Fluorine Chem.*, **72**, 203 (1995).
13. S. V. Kotov, S. D. Pederesen, W. Z.-M. Qui, and D. J. Burton, *J. Fluorine Chem.*, **82**, 13 (1997).
14. S. C. Savett, J. R. Atkins, C. R. Sides, J. L. Harris, B. H. Thomas, S. E. Creager, W. T. Pennington, and D. D. DesMarteau, *J. Electrochem. Soc.*, **149**, A1527 (2002).
15. W. Liu, K. Ruth, and G. Rusch, *J. New Mater. Electrochem. Syst.*, **4**, 227 (2001).
16. R. B. Hogdon, *J. Polym. Sci., Part A: Gen. Pap.*, **6**, 171 (1968).
17. A. E. Steck and C. Stone, in *Proceedings of the 2nd International Symposium on New Materials for Fuel Cell and Modern Battery Systems*, O. Savagodo, P. R. Roberge, and T. N. Veziroglu, Editors, Montreal, Quebec, Canada, July 6-10, 1997, 792 (1997).
18. M. Rikukawa and K. Sanui, *Prog. Polym. Sci.*, **25**, 1463 (2000).
19. O. Savagodo, *J. New Mater. Electrochem. Syst.*, **1**, 66 (1998).
20. J. E. McGrath, in *Proceedings of Advances in Materials for Proton Exchange Membrane Fuel Cell Systems*, Feb. 23-27, ACS, Pacific Grove, CA (2003).
21. F. Wang, M. Hickner, Y. S. Kim, T. A. Zawodzinski, and J. E. McGrath, *J. Membr. Sci.*, **197**, 231 (2002).
22. R. F. Savinell, J. S. Wainright, and M. Litt, in *Proton Conducting Membrane Fuel Cells II*, S. Gottesfeld and T. F. Fuller, Editors, PV 98-27, p. 81, The Electrochemical Society Proceedings Series, Pennington, NJ (1999).
23. R. Savinell, E. Yeager, D. Tryk, U. Landau, J. Wainright, D. Weng, K. Lux, M. Litt, and C. Rogers, *J. Electrochem. Soc.*, **141**, L46 (1994).
24. M. Doyle, S. K. Choi, and G. Proulex, *J. Electrochem. Soc.*, **147**, 34 (2000).
25. S. Chandra, in *Superionic Solids and Solid Electrolytes Recent Trends*, A. L. Laskar and S. Chandra, Editors, p. 190, Material Science Series, Academic Press, Inc., New York (1989).
26. P. Costamagna, C. Yang, A. B. Bocarsly, and S. Srinivasan, *Electrochim. Acta*, **47**, 1023 (2002).
27. V. Ramani, H. R. Kunz, and J. M. Fenton, *J. Membr. Sci.*, **232**, 31 (2004).
28. M. Watanabe, H. Uchida, Y. Seki, M. Emori, and P. Stonehart, *J. Electrochem. Soc.*, **143**, 3847 (1996).
29. M. Watanabe, H. Uchida, Y. Seki, and M. Emori, *J. Phys. Chem. B*, **102**, 3129 (1998).
30. H. Uchida, Y. Ueno, H. Hagihara, and M. Watanabe, *J. Electrochem. Soc.*, **150**, A57 (2003).
31. C. Yang, P. Costamagna, S. Srinivasan, J. Benziger, and A. B. Bocarsly, *J. Power Sources*, **103**, 1 (2001).
32. Y. Si, J. M. Fenton, and H. R. Kunz, Abstract 116, The Electrochemical Society Meeting Abstracts, Vol. 2000-1, Washington, DC, March 25-29, 2001.
33. Y. I. Park, J. D. Kim, and M. Nagai, *J. Mater. Sci. Lett.*, **19**, 1621 (2000).
34. M. A. Harmer and Q. Sun, U.S. Pat. 6,515,190 (2003).
35. K. T. Adjemian, S. J. Lee, S. Srinivasan, J. Benziger, and A. B. Bocarsly, *J. Electrochem. Soc.*, **149**, A256 (2002).
36. K. T. Adjemian, S. Srinivasan, J. Benziger, and A. B. Bocarsly, *J. Power Sources*, **109**, 356 (2002).
37. K. A. Mauritz, I. D. Stefanithis, S. V. Davis, R. W. Scheez, R. K. Pope, G. L. Wilkes, and H. H. Huang, *J. Appl. Polym. Sci.*, **55**, 181 (1995).
38. W. G. Grot and G. Rajendran, U.S. Pat. 5,919,583 (1999).
39. S. M. J. Zaidi, S. D. Mikhailenko, G. P. Robertson, M. D. Guiver, and S. Kaliaguine, *J. Membr. Sci.*, **173**, 17 (2000).
40. F. Lonyi, J. Valyon, J. Engelhardt, and F. Mizukami, *J. Catal.*, **60**, 279 (1996).
41. M. Misono and T. Okuhara, *CHEMTECH*, **23**, (1993); M. Misono, T. Okuhara, and N. Mizuno, *Successful Design of Catalysts*, T. Inui, Editor, p. 267, Elsevier, Amsterdam (1988).
42. G. A. Olah, G. K. Surya Prakash, and J. Sommer, *Superacids*, Wiley, New York (1985).
43. K. Kanamura, H. Morikawa, and T. Umegaki, *J. Electrochem. Soc.*, **150**, A193 (2003).
44. T. Thampan, S. Malhotra, H. Tang, and R. Datta, *J. Electrochem. Soc.*, **147**, 3242 (2000).
45. E. A. Mason and A. P. Malinauskas, *Gas Transport in Porous Media: The Dusty Gas Model*, p. 142, Elsevier, Amsterdam (1983).
46. P. Choi and R. Datta, *J. Electrochem. Soc.*, **150**, E601 (2003).
47. K. Arata, *Appl. Catal., A* **146**, 3 (1996).
48. R. B. Moore and C. R. Martin, *Anal. Chem.*, **58**, 2570 (1986).
49. W. Apichatachutapan, R. B. Moore, and K. A. Mauritz, *J. Appl. Polym. Sci.*, **62**, 417 (1996).
50. P. Liu, J. Bandara, Y. Lin, D. Elgin, L. F. Allard, and Y. P. Sun, *Langmuir*, **18**, 10398 (2002).
51. J. E. Resoke and M. A. Barteu, *J. Phys. Chem. B*, **101**, 1113 (1997).
52. E. Busenberg and C. V. Clemency, *Clays Clay Miner.*, **21**, 213 (1973).
53. W. B. Johnson and L. Wen, in *High Temperature Materials Symposium in Honor of the 65th Birthday of Professor Wayne L. Worrell*, S. C. Singhal, Editor, PV 2002-5, p. 132, The Electrochemical Society Proceedings Series, Pennington, NJ (2002).
54. B. Bahar, C. Cavalca, S. Cleghorn, J. Kolde, D. Lane, M. Murthy, and G. Rusch, *J. New Mater. Electrochem. Syst.*, **2**, 179 (1999).
55. T. J. Schmidt, H. A. Gasteiger, G. D. Stäb, P. M. Urban, D. M. Kolb, and R. J. Behm, *J. Electrochem. Soc.*, **145**, 2354 (1998).
56. P. Choi, N. Jalani, and R. Datta, *J. Electrochem. Soc.*, Submitted.
57. N. Miyake, J. S. Wainright, and R. F. Savinell, *J. Electrochem. Soc.*, **148**, A898 (2003).
58. T. Thampan, S. Malhotra, J. Zhang, and R. Datta, *Catal. Today*, **67**, 15 (2001).
59. S. J. Lee, S. Mukerjee, E. A. Ticianelli, and J. McBreen, *Electrochim. Acta*, **44**, 3283 (1999).